EASR

Engineering and Applied Science Research

https://www.tci-thaijo.org/index.php/easr/index

Published by the Faculty of Engineering, Khon Kaen University, Thailand

Parametric study on contribution of combined confining steel and steel fiber to column's displacement ductility

Slamet Widodo[1)], Bambang Sabariman*[2)] and Tavio[3)]

[1)]Department of Civil Engineering and Planning, Universitas Negeri Yogyakarta, 55281, Indonesia
[2)]Department of Civil Engineering, Universitas Negeri Surabaya, 60231, Indonesia
[3)]Department of Civil Engineering, Institut Teknologi Sepuluh Nopember, Surabaya, 60111, Indonesia

Received 20 February 2024
Revised 13 April 2024
Accepted 20 May 2024

Abstract

This study examines the contribution of confinement with variations in spacing s_h = (50, 65, and 80) mm and concrete reinforced with steel fiber to displacement ductility. Eight test column specimens (No. 1, 2, 3, 6, 7, 8, 11, and 12) were also reinforced with stirrups according to ACI 318M:19 provisions while four test column specimens (No. 4, 5, 9, and 10) deliberately reinforced with a slightly wider spacing of stirrups with different yield strengths (f_y) (lower than the code requirements). However, the volumetric ratio of the steel fiber was varied, i.e. V_f = 0%, 0.5%, 1%, 1.5%, and 2%. The column was then subjected to a quasi-cyclic and a constant axial load of $P_a = 0.121.A_g.f_c'$. The test results indicated that all test column specimens could attain the full ductile/fully ductile criteria since μ_Δ>4. When the drift ratio required by ACI 318M-19 is observed, the use of combined confining stirrups and steel fiber works together simultaneously to achieve a drift ratio capacity that exceeds the minimum required target of 3%, meaning that the columns could perform satisfactorily.

Keywords: Confinement, Disaster risk reduction, Drift ratio, Ductility, Quasi-cyclic, Steel fiber

1. Introduction

Structural beams are very important to be designed to have adequate strength and ductility [1, 2]. However, structural columns are even more important members of building structures because they must sustain axial loads and lateral loads simultaneously, such that the demand for ductility must be adequate. The ductility value (μ_Δ) is considered based on the ultimate displacement value (Δ_u) divided by the displacement at first yielding (Δ_y). It must be evaluated whether it has reached a certain ductility criterion according to the code [3]. If the value of μ_Δ is less than 2 then it can be defined as Low Ductility Demand, if 2 to 4 is defined as Moderate Ductility Demand, and if greater than 4 is defined as High Ductility Demand/full ductile. The μ_Δ value is taken from the drift ratio value at $0.80P_{max}$ or when there is a 20% reduction in strength after the maximum load [4]. The code also requires that the column must be able to achieve a drift ratio of 3% without experiencing a drastic reduction in strength, which means the column must be ductile.

Achieving ductility can be done by providing confinement in the form of stirrups in the concrete [5-13] or many others [14-17]. Particularly for seismic-resistant structures, they are usually confined using densely-spaced stirrups. This condition causes the detailing to become congested, resulting in harder implementation on site.

Currently, the use of higher concrete strength has also been widely used, including the use of steel fiber in several structural elements [18-22] its use is based on volumetric fiber V_f between 0.5% and 2%, the results show an increase in the strength of the structural members.

Based on the above discussion, the study aims to find the contribution from the combination of confinement values according to [8] and the use of steel fiber. The confinement in the study used square stirrups with a diameter of D8 mm with various spacings (s_h = 50, 65, and 80 mm). To improve the performance, steel fiber was introduced according to the volumetric ratio with intermediate values, namely V_f = 0%, 0.5%, 1%, 1.5%, and not more than 2%. It was observed that the drift ratio was achieved at 3% under inelastic conditions and the ductility was satisfactory.

The primary aim of the study is to investigate the contribution of steel fiber in combination with confining steel to the displacement ductility of concrete columns due to combined axial and lateral cycling loads. The contribution of steel fiber in reducing the need for stirrups as confinement in columns has been found to significantly alleviate the congestion of steel reinforcement in concrete columns required by the seismic code provisions in achieving comparable performances.

2. Materials and methods

This research was carried out in the laboratory by making twelve column test specimens. The column confinement used was square stirrups with spacings s_h = 50, 65, and 80 mm. The concrete used was normal-strength concrete. The concrete was then reinforced with

*Corresponding author.
Email address: bambangsabariman@unesa.ac.id
doi: 10.14456/easr.2024.44

steel fiber with the volumetric ratio (V_f), while the main reinforcement ratio of the column A_{st} = 2.48%. Column cross-sectional dimensions b×h = 200×200 mm and column height L = 800 mm. Columns were designed with FSSR < 0.6 [23]. This ratio was chosen such that the column collapses due to flexural failure. The columns were tested under quasi-cyclic loading with a $P_{axial\text{-}constant}$ load = $0.121A_g f'_c$ and a horizontal load P_h starting from zero until the column collapsed. The test adopted the displacement-controlled method, then analyzed for achieving a drift ratio of 3% in post-peak load conditions of $0.8P_{h\text{-}max}$ and also analyzed if the ductility is achieved.

This research also observed the effect of using $A_{sh\text{-}provided} < A_{sh\text{-}ACI}$, namely column test specimens No. 4-5 and 9-10, where Ash-provided should be at least the same as $A_{sh\text{-}ACI}$. This was conducted to find how far the contribution of stirrups and steel fiber when used simultaneously as concrete reinforcement, particularly for reinforced concrete columns.

2.1 Materials and specimens

The concrete used in this research is normal strength concrete with $f'_{c\text{-}target}$ = 25 MPa produced by the manufacturer. This option was selected such that the consistency of the concrete strength was uniform and thus, the designed strength target was attained. However, the details of material use in the mix design are still given in Table 1. Likewise, the steel fiber used is also provided by the manufacturer with a double hook shape. The amount used was based on volumetric ratio, namely (V_f) = 0%, 0.5%, 1%, 1.5%, and 2%.

Table 1 Mix design for a volume of 1 m^3 of concrete with f'_c of 25 MPa

No.	Materials	1 m^3 SSD (kg/m^3)
1.	Cement, OPC type 1	322
2.	Fly ash, ex. Jepara (Indonesia)	57
3.	Sand, ex. Merapi (Indonesia)	823
4.	Coarse Agg, ex. Merapi (Indonesia) split size 10-20 mm	962
5.	Water	170
6.	Admixture, Sika VZ (in Indonesia)	1,22
	Density	2335

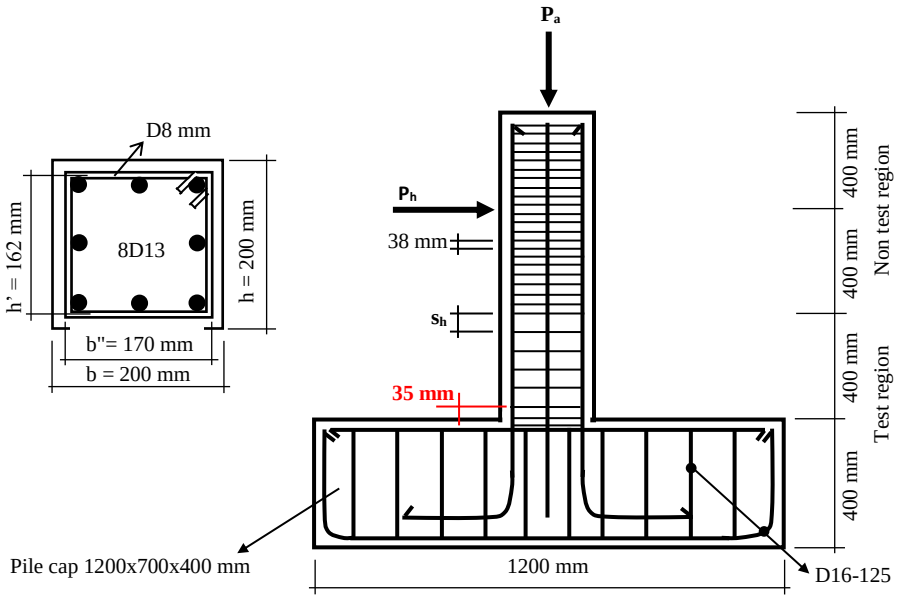

Figure 1 Details of column reinforcement

Figure 2 Column reinforcement cage and steel fiber used with aspect ratio l/d = 80

The reinforcing steel used was D8 mm for square stirrups and D13 mm for the main column reinforcement, while the pile cap was strengthened using reinforcement using D16 mm with a spacing of 125 mm. This pile cap was designed to be as strong as possible so that failure did not occur in the pile cap region. Concrete reinforcement design, such as spacing of stirrups at s_h = 50, 65, and 80 mm, was intended such that the column reaches full ductility of μ_Δ>4 [3, 8].

The combination of using stirrups, main reinforcement, and a constant axial load of P_a=0.121$A_g f'_c$ was also intended such that all columns reached FSSR<0.6 [23]. This condition aims to prevent damage to plastic joints due to bending. Based on this design, the column reinforcement and anchorage were made as in Figures 1 and 2 [24] with detailed column test specimens given in Table 2.

Table 2 Details of column test specimens

No.	Specimen ID	b=h (mm)	L (mm)	Main reinforcement	Stirrups		V_f steel fiber	f_y (MPa)	f_{yh} (MPa)	$f'_{c\text{-average}}$ (MPa)	$A_{sh\text{-}1\text{-}ACI}$ (mm^2)	$A_{sh\text{-}2\text{-}ACI}$ (mm^2)	$A_{sh\text{-}provided}$ (mm^2)
					D (mm)	s_h (mm)							
1	Col.2.a	200	800	8D13	8	65	0	405.87	546.83	27	60.02	46.88	93.33
2	Col.3.a	200	800	8D13	8	80	0	405.87	546.83	27	73.87	57.69	93.33
3	Col.1.b	200	800	8D13	8	50	0.5%	317.01	344.30	27	73.45	57.37	86.67
4	Col.2.b	200	800	8D13	8	65	0.5%	317.01	344.30	27	95.48	74.58	86.67
5	Col.3.b	200	800	8D13	8	80	0.5%	317.01	344.30	27	117.52	91.79	86.67
6	Col.2.c	200	800	8D13	8	65	1%	405.87	546.83	27	60.02	46.88	93.33
7	Col.3.c	200	800	8D13	8	80	1%	405.87	546.83	27	73.87	57.69	93.33
8	Col.1.d	200	800	8D13	8	50	1.5%	317.01	344.30	27	73.45	57.37	86.67
9	Col.2.d	200	800	8D13	8	65	1.5%	317.01	344.30	27	95.48	74.58	86.67
10	Col.3.d	200	800	8D13	8	80	1.5%	317.01	344.30	27	117.52	91.79	86.67
11	Col.2.e	200	800	8D13	8	65	2%	405.87	546.83	27	60.02	46.88	93.33
12	Col.3.e	200	800	8D13	8	80	2%	405.87	546.83	27	73.87	57.69	93.33

Note: Col.1= s_h 50 mm, Col.2= s_h 65 mm, Col.3= s_h 80 mm, a=V_f 0%, b=V_f 0.5%, c=V_f 1%, d=V_f 1.5%, e=V_f 2%.

2.2 Experimental works

The experiments in this study were set with a constant axial load on the column of P_a=0.121$A_g f'_c$ and given a horizontal load. This horizontal load was considered to represent the lateral load or earthquake load. The test was carried out using the displacement-controlled method according to the loading pattern as in Figure 3 [25]. The loading pattern was then changed into displacement (drift) form as in Table 3. Table 3 is a reference for carrying out the displacement-controlled test, meaning that the test specimen is given a drift according to Table 3 and then the drift and load that causes the drift are automatically recorded. If the amount of drift has been completed in the test then it is called one phase of testing, but in this test three phases with the same drift are held, after three phases have been passed then one test cycle has occurred. The cycle is stopped if the column has collapsed or plastic joints have appeared in the test area. The steps in Figure 3 are elaborated as follows:

1. The column test specimen is loaded in a displacement-controlled sequence representing drift (Δ). This condition is considered to represent the conditions during an earthquake.
2. Three full cycles should be performed at each drift ratio (see Figure 3).
3. The initial condition of the drift ratio should be in the linear elastic behavior of the column test specimen. The next drift ratio should not be less than 1.25 times, and not more than 1.5 times the previous drift ratio.
4. Testing of column test specimens should be carried out in stages by gradually increasing the drift ratio until a minimum drift ratio value of 0.035 is reached.
5. Data recording of drift (see Table 3) versus horizontal force (P_h) should be carried out continuously to interpret the performance of the column test specimen qualitatively and must be documented.

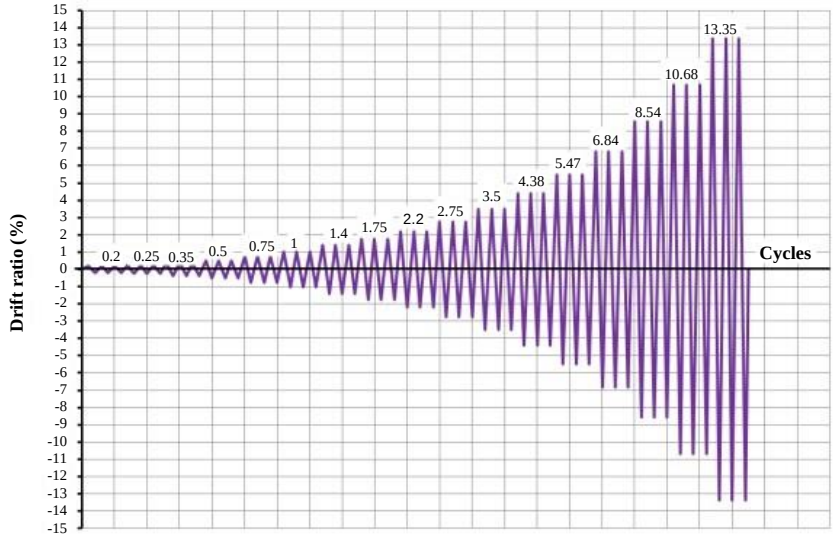

Figure 3 Displacement-controlled loading pattern

Table 3 Drift ratio of L_{column} = 800 mm

Cycle no.	Drift ratio (%)	Displacement (mm)	Cycle no.	Drift ratio (%)	Displacement (mm)
1	0.20	1.60	10	2.75	22.00
2	0.25	2.00	11	3.50	28.00
3	0.35	2.80	12	4.38	35.00
4	0.50	4.00	13	5.47	43.75
5	0.75	6.00	14	6.84	54.69
6	1.00	8.00	15	8.54	68.36
7	1.40	11.20	16	10.68	85.45
8	1.75	14.00	17	13.35	106.81
9	2.20	17.60			

2.3 Test setup for quasi-cyclic loading

The quasi-cyclic column experiment carried out in the laboratory in this study gave a constant axial load of $P_a = 0.121A_g f'_c$ and was also given a horizontal load. The test setup for quasi-cyclic loading using the displacement-controlled method has been designed to be able to properly measure the displacements in Table 3, and the load that occurs. Several data recording devices are connected to the Kyowa brand recorder unit, during testing it is connected directly to the computer. The actual test setup is shown in Figure 4.

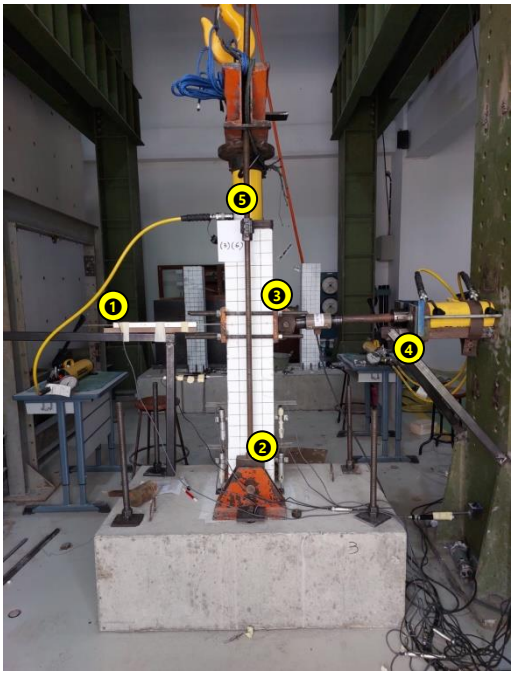

Figure 4 Actual test setup, ❶ = LVDT horizontal, caps. 200 mm, ❷ = LVDT vertical, caps. 50 mm, ❸ = double-acting load cell, caps. 100 kN, ❹ = double-acting hydraulic jack, caps. 200 kN, ❺ = single-acting hydraulic jack, caps. 200 kN.

3. Result and discussion

3.1 Concrete compression test results

The concrete compression test used six concrete cylinders with a diameter of 150 mm and a height of 300 mm. Casting the concrete cylinders was at the same time as casting the column test specimens. After the concrete cylinders were 28 days old, compression tests were then carried out. The results of the compression test are given in Table 4.

Table 4 Compressive strength of concrete

No.	Specimen ID	Compressive strength of concrete (MPa)
1	S_1	26.07
2	S_2	29.95
3	S_3	24.96
4	S_4	26.45
5	S_5	27.80
6	S_6	26.77
	Average	27.00

3.2 Reinforcing steel tensile test results

The tensile test results of D8 stirrup steel reinforcement were found to be f_{yh} = 317.01 and 546.83 MPa, while the tensile tests of longitudinal column reinforcement D13 were found to be f_y = 344.30 and 405.87 MPa. All the reinforcement used, both D8 and D10, had an average elongation value of larger than 11%, meaning the reinforcement was applicable for seismic purposes [4, 26, 27].

3.3 Quasi-cyclic test results of column specimens

After the column test specimens were 28 days old, the quasi-cyclic tests were then carried out as described in the previous explanation. The results were then graphed after which the analyses of the achieved drift ratios and displacement ductility values were carried out. The results are shown in Figure 5 (1-12) and the values are summarized in Table 5.

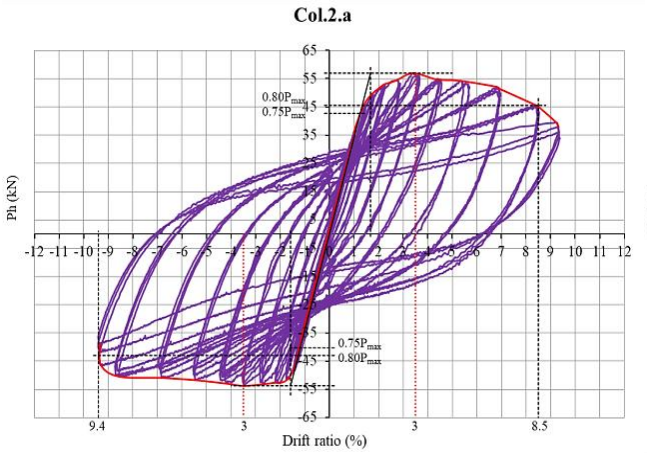

(1) Column s_h=65 mm, V_f=0% (Col.2.a)

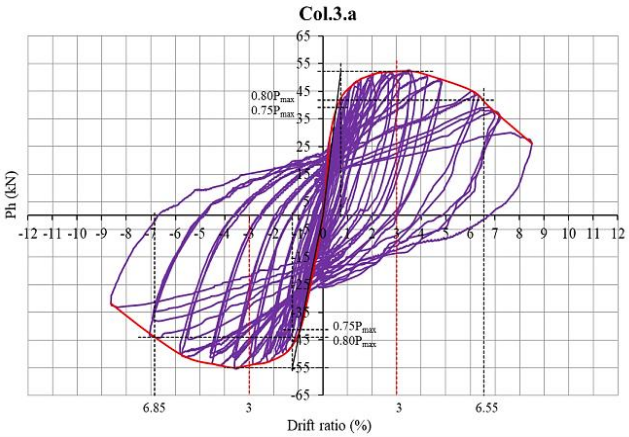

(2) Column s_h=80 mm, V_f=0% (Col.3.a)

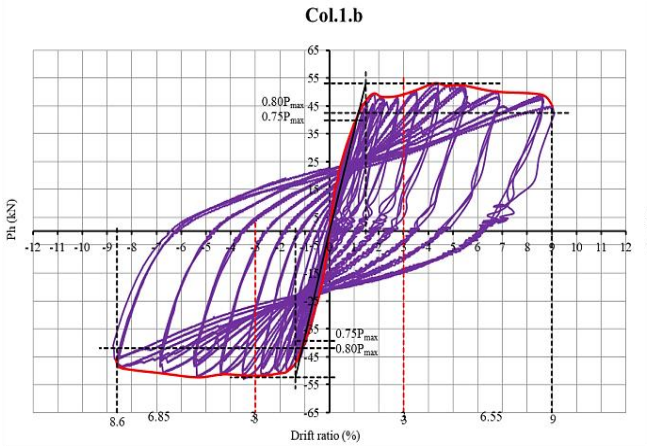

(3) Column s_h=50 mm, V_f=0.5% (Col.1.b)

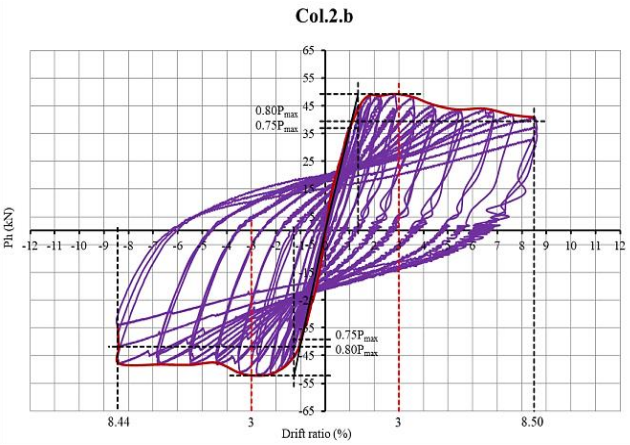

(4) Column s_h=65 mm, V_f=0.5% (Col.2.b)

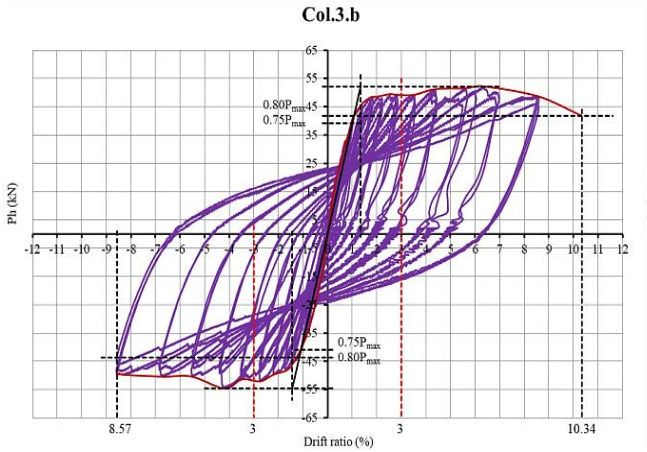

(5) Column s_h=80 mm, V_f=0.5% (Col.3.b)

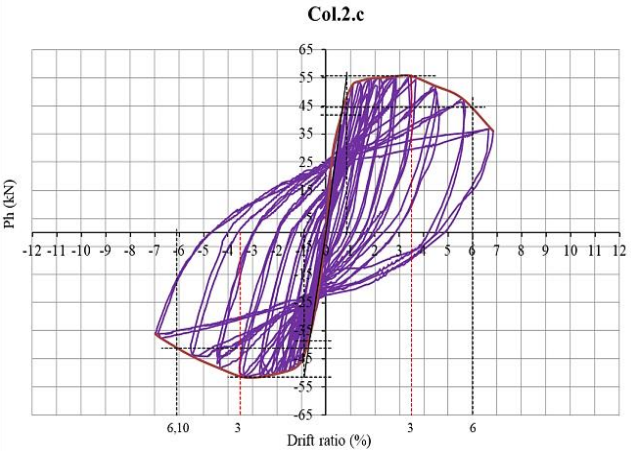

(6) Column s_h=65 mm, V_f=1% (Col.2.c)

Figure 5 Loop hysteresis curve based on drift ratio vs column P_h

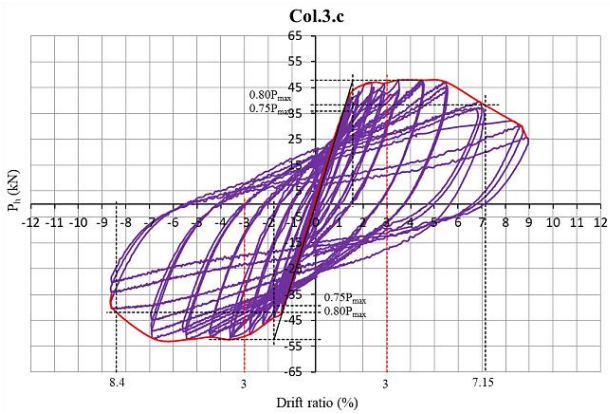

(7) Column s_h=80 mm, V_f=1% (Col.3.c)

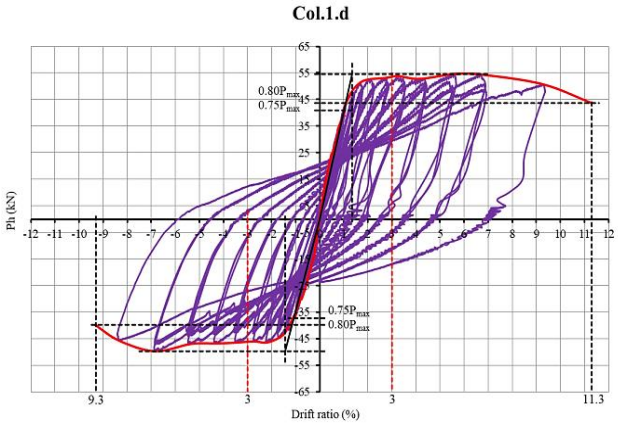

(8) Column s_h=50 mm, V_f=1.5% (Col.1.d)

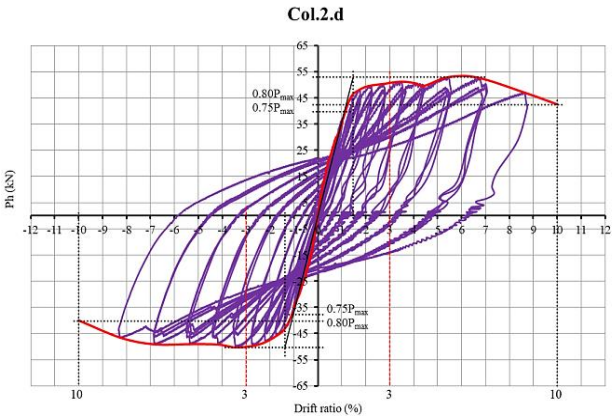

(9) Column s_h=65 mm, V_f=1.5% (Col.2.d)

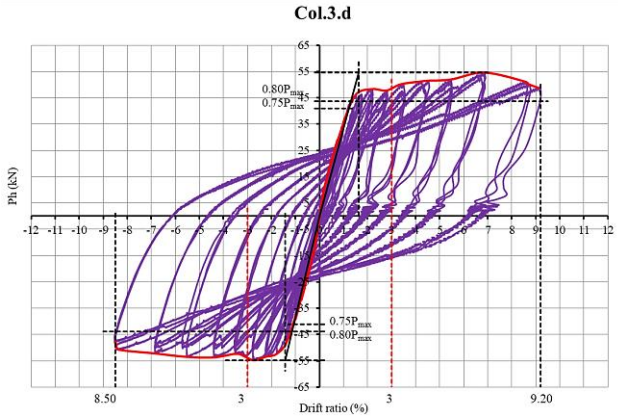

(10) Column s_h=80 mm, V_f=1.5% (Col.3.d)

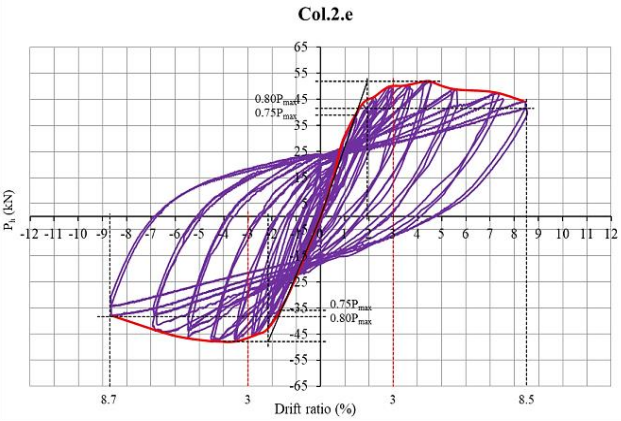

(11) Column s_h=65 mm, V_f=2% (Col.2.e)

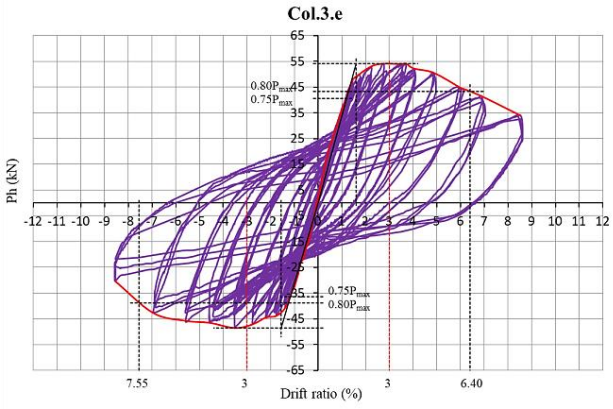

(12) Column s_h=80 mm, V_f=2% (Col.3.e)

Figure 5 (continued) Loop hysteresis curve based on drift ratio vs column P_h

Table 5 Recapitulation of experimental results $\mu_{\Delta\text{-exp}}$ at $0.80P_{max}$

No.	Specimen ID	$\mu_{\Delta\text{-exp}}$ compression (mm)	$\mu_{\Delta\text{-exp}}$ tension (mm)	$\mu_{\Delta\text{-exp}}$ average (mm)	Criteria	Drift ratio$_{exp}$ compression (%)	Drift ratio$_{exp}$ tension (%)	Drift ratio$_{exp}$ average (%)
1.	Col.2.a	5.95	5.09	5.52	Full ductile	9.40	8.50	8.95
2.	Col.3.a	5.50	9.03	7.27	Full ductile	6.85	6.55	6.70
3.	Col.1.b	6.23	6.12	6.18	Full ductile	8.60	9.00	8.80
4.	Col.2.b	6.65	6.34	6.50	Full ductile	8.44	8.50	8.47
5.	Col.3.b	5.95	7.70	6.82	Full ductile	8.57	10.34	9.45
6.	Col.2.c	6.85	7.06	6.96	Full ductile	6.10	6.00	6.05
7.	Col.3.c	4.77	4.58	4.68	Full ductile	8.40	7.15	7.78
8.	Col.1.d	6.46	8.41	7.43	Full ductile	9.30	11.30	10.30
9.	Col.2.d	7.25	6.80	7.02	Full ductile	10.00	10.00	10.00
10.	Col.3.d	5.94	5.64	5.79	Full ductile	8.50	9.20	8.85
11.	Col.2.e	4.01	4.40	4.21	Full ductile	8.70	8.50	8.60
12.	Col.3.e	4.84	4.00	4.42	Full ductile	7.55	6.40	6.98

Note: Col.1= s_h 50 mm, Col.2= s_h 65 mm, Col.3= s_h 80 mm, a=V_f 0%, b=V_f 0.5%, c=V_f 1%, d=V_f 1.5%, e=V_f 2%.

Based on Figure 5, the loop hysteresis envelope curve is depicted (see Figure 6) which is grouped based on volumetric steel fiber and stirrup spacing. Figure 6 shows the difference in drift ratio vs. P_h among twelve column test specimens. It can be seen that the largest displacement was attained by column test specimen Cl.1.d, while the smallest displacement was achieved by column test specimen Cl.2.c. However, all twelve column test specimens were in full ductile criteria (see Table 5). Figure 6 also shows that the displacement of the column test specimen with s_h = 80 mm is seen to be in the middle of all twelve column test specimens, meaning that the column test specimen with s_h = 80 mm can be said to be in a conservative condition (safe condition), so it does not need to be designed using stirrups with s_h = 50mm. This can be beneficial in the process of constructing the concrete column members because the work will be less complicated. Apart from that it can be understood that the design and implementation of concrete construction might deviate and be an issue on site. All twelve column test specimens have conformed to the requirements of ACI 318M-19, i.e. the drift ratio has exceeded 3% at $0.8P_{h\text{-}max}$. Figure 5 shows the column test specimen's capabilities to withstand the horizontal load P_h, ranging from 47.87 to 56.95 kN. However, their capability to experience lateral displacement at $0.80P_{h\text{-}max}$ varied. This drift is very important to consider because it is an inseparable part of the ACI 318M-19 requirement that after the post-elastic response at $0.80P_{h\text{-}max}$, it should be able to sustain at least a 3% drift ratio. In this research, it turns out that the column test specimen with s_h = 80 mm was still able to sustain a displacement equivalent to the column test specimen with s_h = 50 mm. Thus, it indicates that the co-existence of both steel fiber and stirrups as confinement has a significant impact on displacement ductility. This is because the displacement ductility at the highest/lowest tension or highest/lowest compression has exceeded the drift ratio limit of 3%.

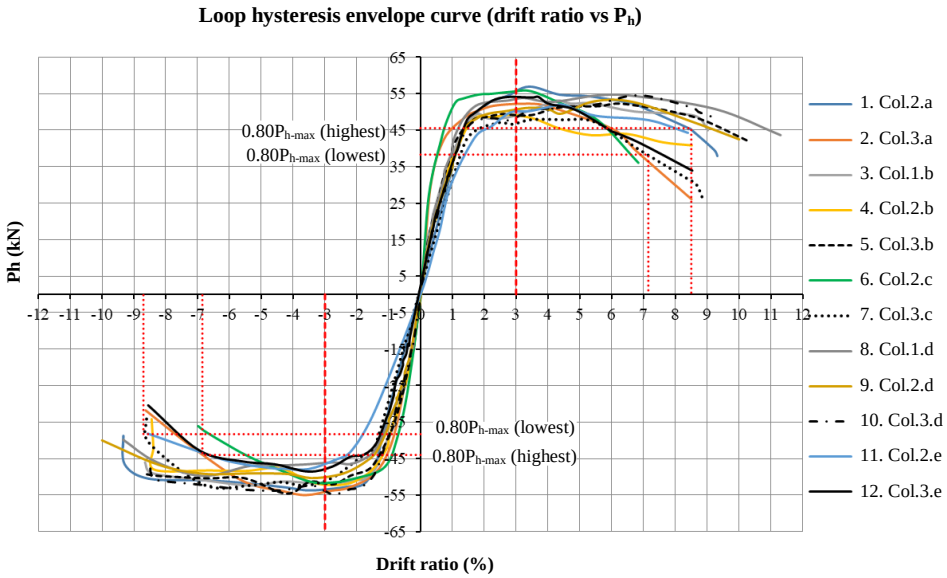

Figure 6 Backbone curves of the hysteretic loops from test column specimens

Some of the data mentioned above are then discussed using the reference of Elwood et al. [28]. This is also a reference to ACI 318-19 [4] which is automatically included in article R18.7.5.4 SNI 2847:2019 [29]. It is stated that the column must be able to achieve a drift ratio of 3% without experiencing a drastic reduction in strength. The reduction in question is $0.8P_{h\text{-}max}$ in inelastic conditions.

Figure 7 shows the column drift ratio capacity between the A_{sh} ratio of the installed confining reinforcement ($A_{sh\text{-}test}$) to the confining reinforcement based on ACI ($A_{sh\text{-}ACI}$). It also shows the column drift ratio capacity as a function of concrete confinement and displays the column performance target represented by the horizontal line in drift ratio of 3%.

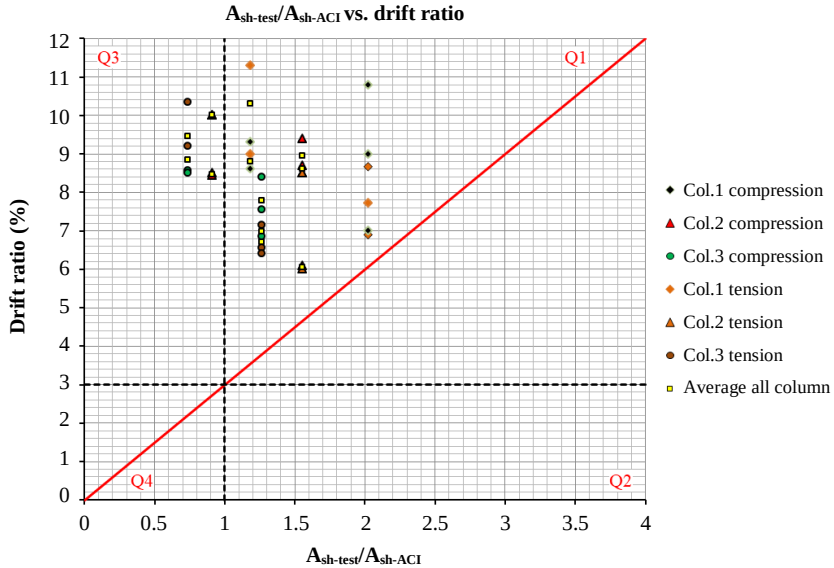

Figure 7 Relationship between stirrup area ratio vs. drift ratio [28, 29]

In Figure 8, data in quadrant 1 (Q1) is a column with constraints that exceed ACI requirements but have a drift capacity that is the same or greater than the performance target (≥3%). Data in quadrant 4 (Q4) represents columns with less confinement gain than the ACI requirement but with drift capacity less than the performance target. The data appearing in the upper left quadrant 3 (Q3) represents columns with confining reinforcement that is less than the ACI requirement but shows a drift capacity that exceeds the target, thus indicating that the results in Q3 can be considered very conservative. In contrast, the data in the lower right quadrant 2 (Q2) represents columns with more confinement than required by the provisions but shows a drift capacity below the target, so the results in Q2 can be considered not conservative. The confinement conditions above the red line in Q2 show a trend of proportional increase in drift due to the increase in Ash usage, where it can be seen that all experimental columns Col.1, Col. 2, and Col. 3 have shown confinement results that can be categorized as ideal and Col. 1 shows a relatively higher drift. However, if you look at the results of the displacement ductility test, all groups of test specimens have entered the full ductile criteria (μ_Δ>4), however, several test specimens are in Q3, this is because the Ash-provided are less than the $A_{sh\text{-}ACI}$ value so the condition very conservative.

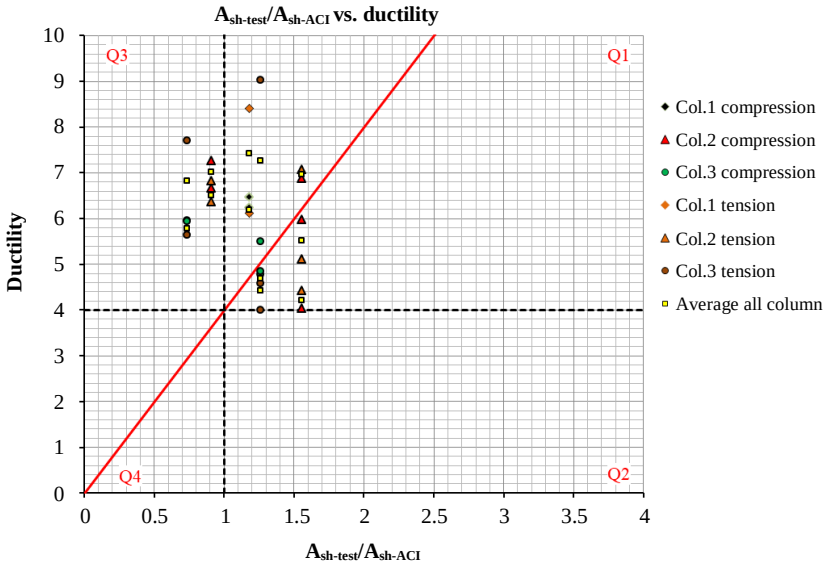

Figure 8 Relationship of A_{sh} vs. displacement ductility (μ_Δ)

4. Conclusion

In this research, the combination of stirrups and steel fiber shows that:

- Columns confined by stirrups with a distance of s_h = 50, 65, and 80 mm and using V_f = 0%, 0.5%, 1%, 1.5%, and 2% all have the same drift ratio capacity or even greater than the drift ratio performance target of ≥3% so that the use of s_h = 80 mm and adding a certain V_f can be said to be in fairly conservative conditions, at least conforming the requirements of ACI 318-19 or R18.7.5.4 SNI 2847:2019.
- In Figure 7, the column test specimen is in the upper right quadrant 1 (Q1). This indicates that the confinements are in ideal conditions so that the stirrup distance can be reduced from s_h = 50 mm to s_h = 80 mm.
- The achievement of ductility in the study can also be said to be quite conservative, where all the test specimens entered the full ductile criteria, so it can also be said that the stirrup confinement with a distance of s_h = 80 mm reinforced with steel fiber have satisfied the demands of ductility requirements, so there is no need to use s_h = 50 mm.
- The use of installed stirrups should be at least the same as $A_{sh\text{-}ACI}$, but several column test specimens in this study have been tested with $A_{sh\text{-}provided}$<$A_{sh\text{-}ACI}$ and reinforced with steel fiber in columns with A_{sh}<$A_{sh\text{-}ACI}$, the results show that the ductility achieved is still within the full criteria ductile, this indicates that steel fiber contributes to column strength, such as the achievement of column numbers 4-5 and 9-10 in this study.

5. Acknowledgment

The authors express their sincere gratitude for all the funding received from the 2023 Indonesian Collaborative Research Grant, under ITS with contract no. 1662/PKS/ITS/2023, UNESA with contract no. B/38242/UN38.III.1/LK.04.00/2023, and UNY with contract no. T/9.1.8/UN/34.9/PT.01.03/2023. The authors also gratefully acknowledge the financial support received from the Institut Teknologi Sepuluh Nopember for this work, under the project scheme of the Publication Writing and IPR Incentive Program (PPHKI) 2024.

6. References

[1] Anggraini R, Tavio, Raka IGP, Agustiar. Experimental load-drift relations of concrete beam reinforced and confined with high-strength steel bars under reversed cyclic loading. ASEAN Eng J. 2021;11(4):56-69.
[2] Anggraini R, Tavio, Raka IGP, Agustiar. Flexural capacity of concrete beams reinforced with high-strength steel bars under monotonic loading. Int J GEOMATE. 2021;20(77):173-80.
[3] Federal Emergency Management Agency. FEMA 356/November 2000. Prestandard and commentary for the seismic rehabilitation of buildings. Washington: American Society of Civil Engineers, Federal Emergency Management Agency; 2000.

[4] ACI Committee 318. Building code requirements for structural concrete (ACI 318-19), commentary on building code requirements for structural concrete (ACI 318R-19). Farmington Hills: American Concrete Institute; 2019.
[5] Seong DJ, Kim TH, Oh MS, Shin HM. Inelastic performance of high-strength concrete bridge columns under earthquake loads. J Adv Concr Technol. 2011;9(2):205-20.
[6] Cusson D, Paultre P. Stress-strain model for confined high-strength concrete. J Struct Eng. 1995;121(3):468-77.
[7] Mander JB, Priestley MJN, Park R. Theoretical stress-strain model for confined concrete. J Struct Eng. 1988;114(8):1804-26.
[8] Scott BD, Park R, Priestley MJN. Stress-strain behavior of concrete confined by overlapping hoops at low and high strain rates. ACI J Proc. 1982;79(1):13-27.
[9] Park R, Paulay T. Reinforced concrete structures. New York: John Wiley & Sons; 1975.
[10] Agustiar, Tavio, Raka IGP, Anggraini R. Behavior of concrete columns reinforced and confined by high-strength steel bars. Int J Civ Eng Technol. 2018;9(7):1249-57.
[11] Machmoed SP, Tavio, Raka IGP. Potential of new innovative confinement for square reinforced concrete columns. J Phys: Conf Ser. 2020;1469:012027.
[12] Machmoed SP, Tavio, Raka IGP. Performance of square reinforced concrete columns confined with innovative confining system under axial compression. Int J GEOMATE. 2021;21(85):137-44.
[13] Tavio, Machmoed SP, Raka IGP. Behavior of square RC columns confined with interlocking square spiral under axial compressive loading. Int J Eng Appl. 2022;10(5):322-35.
[14] Pudjisuryadi P, Tavio, Suprobo P. Axial compressive behavior of square concrete columns externally collared by light structural steel angle sections. Int J Appl Eng Res. 2016;11(7):4655-66.
[15] Pinto D, Tavio, Raka IGP. Axial compressive behavior of square concrete columns retrofitted with GFRP straps. Int J Civ Eng Technol. 2019;10(1):2388-400.
[16] Khatulistiani U, Tavio, Raka IGP. Influence of steel bars for external confinement on compressive strength of concrete. Int J GEOMATE. 2021;20(82):146-52.
[17] Honestyo A, Tavio, Ardhyananta H. Axial compressive behavior of bubble-size plastic straw waste FRP-confined circular concrete. Int J Eng Appl. 2023;11(2):73-80.
[18] Mansur MA, Chin MS, Wee TH. Stress-strain relationship of high-strength fiber concrete in compression. J Mater Civ Eng. 1999;11(1):21-9.
[19] Shakya K, Watanabe K, Matsumoto K, Niwa J. Application of steel fibers in beam-column joints of rigid-framed railway bridges to reduce longitudinal and shear rebars. Constr Build Mater. 2012;27(1):482-9.
[20] Eltobgy HH. Structural design of steel fiber reinforced concrete in-filled steel circular columns. Steel Compos Struct. 2013;14(3):267-82.
[21] Sabariman B, Soehardjono A, Wisnumurti, Wibowo A, Tavio. Stress-strain behavior of steel fiber-reinforced concrete cylinders spirally confined with steel bars. Adv Civ Eng. 2018;2018:1-8.
[22] Sabariman B, Soehardjono A, Wisnumurti, Wibowo A, Tavio. Stress-strain model for confined fiber-reinforced concrete under axial compression. Arch Civ Eng. 2020;66(2):119-33.
[23] American Society of Civil Engineerings. ASCE/SEI 41-0.6: Seismic rehabilitation of existing buildings. USA: ASCE; 2007.
[24] Sabariman B, Sofianto MF. Study of crack patterns in the beam column joint due to the upwards anchoring beam effect. AIP Conf Proc. 2017;1855(1):040004.
[25] ACI Committee 374. ACI 374.1-05 (Reapproved 2014): acceptance criteria for moment frames based on structural testing and commentary. Farmington Hills: American Concrete Institute; 2014.
[26] Anggraini R, Tavio, Raka IGP, Agustiar. Stress-strain relationship of high-strength steel (HSS) reinforcing bars. AIP Conf Proc. 2018;1964:020025.
[27] National Standardization Agency of Indonesia. SNI 2052:2017, concrete reinforcing steel. Jakarta: National Standardization Agency (Badan Standardisasi Nasional); 2017. (In Indonesian)
[28] Elwood KJ, Maffei J, Riederer KA, Telleen K. Improving column confinement-part 2: proposed new provisions for the ACI 318 building code. Concr Int. 2009:41-8.
[29] National Standardization Agency of Indonesia. SNI 2847:2019, structural concrete requirements for buildings. Jakarta: National Standardization Agency (Badan Standardisasi Nasional); 2019. (In Indonesian)